CONSTRAINTS ON THE PROPOSED FORMATION MODELS FOR MARTIAN CENTRAL PIT CRATERS. N. G. Barlow, Dept. Physics and Astronomy, NAU Box 6010, Northern Arizona University, Flagstaff, AZ 86011-6010. Nadine.Barlow@nau.edu.

Introduction: Impact craters with central pits are common on Mars, Ganymede, and Callisto but rare elsewhere in the solar system. Central pit craters display a central depression, either directly on the crater floor ("floor pit") or atop a central peak ("summit pit") (Fig. 1). Floor pits dominate among central pit craters on Ganymede and Callisto, but Martian central pits are almost equally divided between floor and summit pits. Subsurface volatiles have been implicated in the formation of central pit structures. Four models have been proposed for the formation of central pits on Mars:

- Collapse of a central peak in weak target materials ("central peak collapse model") [1].
- Excavation into layered target materials ("layered target model") [2].
- Vaporization of target ice during crater formation and explosive release of the resulting gas ("ice vaporization model") [3].
- Melting of target ice during crater formation and subsequent drainage of the liquid through subsurface fractures ("melt drainage model") [4].

We have been conducting a study of the distributions and characteristics of Martian central pit craters [5, 6]. Although the study is continuing, our results to date are providing new constraints on the proposed central pit formation models.

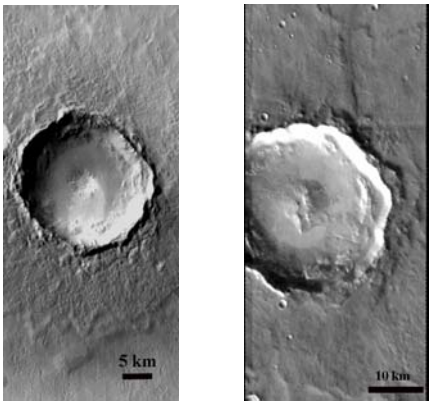

Figure 1: Examples of floor pit (left) and summit pit (right) craters (THEMIS images I11284045 (left) and I24502007 (right)).

Summary of Martian Central Pit Crater Study: We have utilized the Mars Odyssey Thermal Emission Imaging System (THEMIS) daytime IR and VIS imagery to identify and classify Martian central pit craters. Mars Global Surveyor Mars Orbiter Laser Altimeter (MOLA) topography is used to determine the elevation of the pit floor relative to the crater floor. If the floor of the pit lies below the crater floor, the pit is classified as a floor pit. Alternately the pit is classified as a summit pit if the pit floor lies above the crater floor. Our study area currently covers the entire northern hemisphere and the region of the southern hemisphere between 0-30°S 180-330°E. The database currently contains 1312 central pit craters: 899 in the northern hemisphere and 413 in the section of the southern hemisphere thus far investigated. This already exceeds the 1081 central pit craters reported globally from Viking image studies [7]. Out of the 1312 central pit craters in this study, 790 are floor pits and 522 are summit pits.

Floor pit craters range in diameter from 5.0 km (the minimum diameter of this study) to 114.0 km and are found at latitudes up to 68°N. Summit pit craters display a similar diameter (5.1-125.4 km) and latitude (up to 70°N) distribution. Over 75% of central pit craters of both types occur in the 7 to 30 km diameter range. A map showing the distribution of floor and summit pits across the study area suggests that both types of pits occur in similar locations (Fig. 2).

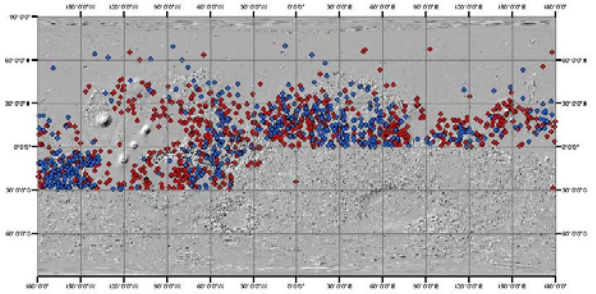

Figure 2: Distribution of floor pits (red) and summit pits (blue).

We tested this suggestion of similar distributions of floor and summit pit craters by producing concentration maps for the northern hemisphere central pit population. We divided the planet into 10° latitude by 10° longitude blocks and normalized the number of central pit craters to the total number of craters in each 10°x10° block. The results suggest that floor pit craters display concentrations within the volcanic plains units of Tharsis, Lunae Planum, Syrtis Major, and Elysium (Fig. 3). Summit pit craters display highest concentrations in the highlands terrain of Arabia Terra (Fig. 4), which is similar to concentration maps of central peaks. Completion of the southern hemisphere survey will allow determination of whether these trends are global.

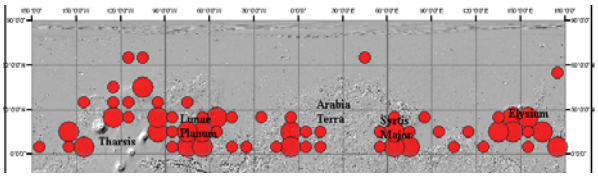

Figure 3: Normalized distribution of floor pit craters in the northern hemisphere of Mars. Larger circules represent >20% concentration of floor pits in a particular 10° latitude by 10° longitude block. Smaller circules represent 10-20% floor pit concentration.

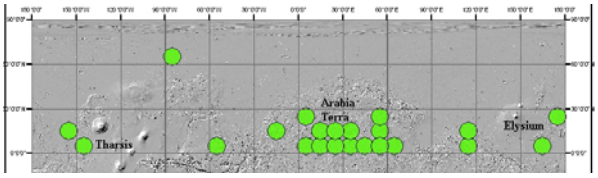

Figure 4: Normalized distribution of summit pit craters in the Martian northern hemisphere. Circules represent 10-20% concentration of summit pits in a particular 10° latitude x 10° longitude block.

Craters containing floor pits display preservational states ranging from 1.0 (heavily eroded) to 7.0 (very fresh crater) using the preservation classification system of Barlow [8]. Summit pit craters range from 1.5 to 7.0. Preservation class is a proxy for crater age, although no direct correspondence between preservation class and absolute age can be derived due to the variety of degradational processes which have operated in different regions and on different time scales across Mars. Nevertheless, the wide range of preservational states for craters containing central pits indicate that central pits have formed over most if not all of Martian history.

The ratio of pit (D_p) to crater (D_c) diameter may provide information about the amount of target ice available when the pit formed. D_p/D_c varies from 0.02 to 0.48 for floor pit craters (median = 0.16) and 0.02-0.29 (median = 0.12) for summit pit craters. This indicates that floor pits are larger relative to their parent crater than summit pits. D_p versus D_c indicates a linear relationship for both floor and summit pits. A linear least squares fit indicates that floor pits follow the relationship $D_p = 0.1572D_c + 0.1245$. Summit pits follow the relationship $D_p = 0.1093D_c + 0.1930$. R^2 values for the floor pit and summit pit D_p vs D_c relationships are 0.7725 and 0.708, respectively.

Constraints on Formation Models: We have compared preliminary results of this study to predictions of the four formation models for central pits. We also have considered recent numerical modeling results for some of these proposed formation mechanisms.

Central peak collapse model: Our results do not support this model for the formation of Martian central pits. The abundance of summit pit and central peak craters in the same regions as floor pit craters indicates that the target material is strong enough for the central peak to resist collapse.

Layered target model: Concentrations of floor pit craters in volcanic plains (Fig. 3), which are likely composed of layered flows, provides some support for this model. However, laboratory experiments which produced central pits for some types of layered targets were small-scale experiments and may not replicate the conditions giving rise to central pits in planetary-scale impact craters.

Ice vaporization model: Most Martian central pit craters occur in the 7- to 30-km-diameter range. Using standard depth-diameter relationships [9], these craters are excavating to depths between 0.7 and 2.5 km, within the region where subsurface ice is expected to exist. Preservational classes of central pit craters indicate that subsurface ice has been present for most if not all of Martian history, and the distribution of central pit craters indicates that subsurface ice is found globally at these depths. These observations are consistent with models of the regional and temporal distribution of subsurface ice [10, 11]. However, the ice vaporization model suffers from the problem of keeping vapor from escaping early in crater formation.

Melt-drainage model: The observations noted in the ice vaporization model discussion also support the melt-drainage model. Numerical modeling of impacts into pure ice targets [12, 13] reproduce the observed crater diameters and D_p/D_c values. The upper diameter limit is constrained by the transition from melt to vapor as impact energy increases, thus explaining the observed diameter ranges. This model also is the only model which predicts both floor and summit pit craters. It is the model best supported by our current data.

Acknowledgements: This work is supported by NASA MDAP award NNX08AL11G.

References: [1] Passey Q.R. and E.M. Shoemaker (1982) *Satellites of Jupiter*, UAz Press, 379-434. [2] Greeley R. et al. (1982) *Satellites of Jupiter*, UAz Press, 340-378. [3] Wood C.A. et al. (1978) *Proc. 9th LPSC*, 3691-3709. [4] Croft S.M. (1981) *LPS XII*, 196-198. [5] Barlow N.G. (2010), *GSA SP 465*, 15-27. [6] Alzate N. and N.G. Barlow (2011) *Icarus*, in press. [7] Barlow N.G. and T.L. Bradley (1990) *Icarus 87*, 156-179. [8] Barlow N.G. (2004) *GRL 31*, L05703. [9] Garvin J.B. et al. (2000) *Icarus 144*, 329-352. [10] Clifford S.M. (1993) *JGR 98*, 10973-11016. [11] Mellon M.T. and B.M. Jakosky (1995) *JGR 100*, 11781-11799. [12] Bray V.J. (2009) PhD Thesis, Imperial College London, 267 pp. [13] Senft L.E. and S.T. Stewart (2011) submitted to *Icarus*.